

## Effects of demi-hull separation ratios on motion responses of tidal current turbines-loaded catamaran

Sony Junianto<sup>1</sup>, Mukhtasor\*<sup>1</sup>, Rudi Walujo Prastianto<sup>1</sup> and Chul Hee Jo<sup>2</sup>

<sup>1</sup>Department of Ocean Engineering, Institut Teknologi Sepuluh Nopember, Kampus ITS Sukolilo 60111, Surabaya, Republic of Indonesia

<sup>2</sup>Department of Naval Architecture and Ocean Engineering, Inha University, 100 Inha-ro, Nam-gu, Incheon, Republic of Korea

(Received June 7, 2019, Revised February 2, 2020, Accepted February 5, 2020)

**Abstract.** Catamaran has recently been a choice to support a typical vertical axis turbine in floating tidal current energy conversion system. However, motion responses associated with the catamaran can reduce the turbines efficiency. The possibility to overcome this problem is to change the catamaran parameter by varying and simulating the demi-hull separations to have lower motion responses. This simulation was undertaken by Computational Fluid Dynamic (CFD) using potential flow analysis. Cases of demi-hull separation were considered, with ratios of demi-hull separation (S) to the breadth of demi-hull (B),  $S/B$  of 3.45, 4.95, 6.45, 7.2 and 7.95. In order to compare to the previous works in the literature, the regular wave was set with wave height of 0.8 m. Furthermore, the analysis was carried out by irregular waves with significant wave height,  $H_s$ , of about 0.09 to 1.5 m and the wave period, T, of about 1.5 to 6 s or corresponding to the wave frequency,  $\omega$ , of about 1.1 to 4.2 rad/s. The wave spectrum was derived from the equation of the International Towing Tank Conference (ITTC). For the case of turbines-loaded catamaran under consideration, the new finding is that the least significant amplitude response can be satisfied at the ratio  $S/B$  of 7.2. This study indicates that selecting a right choice of demi-hull separation ratio could contribute in reducing motion responses of the tidal current turbines-loaded catamaran.

**Keywords:** demi-hull separation; floating turbine; twin turbines; vertical axis; catamaran model; tidal current energy

### 1. Introduction

Tidal current energy can be converted into electricity by using a horizontal or vertical type turbine (Khan *et al.* 2009, Duthoit and Falzarano 2018). Vertical axis turbine has the advantage in responding to every direction of the sea current compared to the horizontal axis turbine (Bachant and Wosnik 2015). The turbine may be supported by a fixed or floating system (Sanchez *et al.* 2014), which is functioned to prop and keep the turbine in a specified site. The floating system is more suitable to extract tidal current energy potentials near the seawater surface (Uihlein and Magagna 2016, Mukhtasor *et al.* 2018, Junianto *et al.* 2018b). In this context, an issue of motion responses of

---

\*Corresponding author, Professor, E-mail: mukhtasor@oe.its.ac.id

the floating structure is very important to consider (Guo *et al.* 2018).

Ma *et al.* (2018) show that motion responses of the floating structure causes interference to the rotation of turbines. For this reason, efforts of reducing the motion responses are directed at securing the high efficiency of the turbine against the motion responses of the floating structure. One of the approaches is to increase average turbine power efficiency by arranging more than one turbine side-by-side (Antheaume *et al.* 2008). The arrangement of several turbines in one platform will change the force or moment which may give better motion responses leading to better turbine efficiency.

A recent study by Li (2014) addresses twin turbines with different arrays. The turbine arrangements in that study are canard layout, tandem layout and 45° diagonal layout which were classified based on the incoming sea current. Among those compared, twin turbines with canard layout have the highest efficiency (Li 2014). Other advantage of arranging twin, or several, turbines in one platform is that the power capacity may be increased in a single of platform.

Another approach of increasing turbine performance is to design a suitable type of the supporting structure. Many researchers have considered a selection of floating structures in order to have better performance in operations. Type of floating tidal current platforms may adopt a technology of ship or unship, e.g., Rho *et al.* (2014), and Ponsoni *et al.* (2018). Rho *et al.* (2014) note that motion responses of semi-submersible are of concern because of its high rotational responses. This in turns may rise problems of fluctuating performance of the turbine (Sheng *et al.* 2016).

Jing *et al.* (2013) and Qasim *et al.* (2018) argue that catamaran has better motion responses than semi-submersible. According to the existing literature (Jing *et al.* 2013, Rho *et al.* 2014, Wang *et al.* 2016a, b, Qasim *et al.* 2018), catamaran is a structure that is suitable for use as the supporting structure in a floating tidal current energy conversion system. However, the use of catamaran for the supporting structure constantly influences the rotation of turbines (Ma *et al.* 2018). Wang *et al.* (2016b) show that the roll motion which was simulated by varying the amplitude gives an influence on the rotation of tidal current turbine. Furthermore, the yaw motion changes the distribution of fluid velocity around the turbine and reduces the turbine efficiency (Wang *et al.* 2016a).

Considering a catamaran in a tidal current energy system, it is worth to underline that the catamaran undergoes a change in the geometry with adding turbine loads. When operated in the marine environment, additional number of turbine in the catamaran will result in a change of behavior of the catamaran in terms of motion responses resulted from the wave excitation. This is the significant difference between a turbines-loaded catamaran and a conventional catamaran.

In order to have lower motion responses, a conventional catamaran, which is a twin-hulls ship, has been analyzed with varying the distance between two demi-hulls (Centeno *et al.* 2001, Jahanbakhsh *et al.* 2009, Danisman 2014). They show that demi-hull separation ratios significantly influence the motion responses of the conventional catamaran. This rises a possibility that a turbines-loaded catamaran may also change its motion responses with changes in demi-hull separation ratios.

This paper analyses the effect of turbine loads and demi-hull separation ratios to the motion responses of the catamaran. Cases of turbine load were considered by varying catamaran in loading without turbine, single turbine, twin turbines. Then, demi-hull separation cases were analyzed by taking variations of the ratio of demi-hull separation to the breadth of the demi-hull. A CFD was employed to analyze the motion responses of the catamaran. The cases are analyzed with regular and irregular waves according to the strait environment. The results are reported in Response Amplitude Operator (RAO), response spectra and significant amplitude of rotational motions.

## 2. Parametric variations

Catamaran has a better motion response as a supporting structure than semisubmersible (Jing *et al.* 2013, Qasim *et al.* 2018), however according to the experiment of Ma *et al.* (2016), the structure has a high frequency vibration, associated with the motion response. This study considers the catamaran (Ma *et al.* 2016) as a base design causing the turbine fluctuation which is harmful to the turbine (Sheng *et al.* 2016). To find a lower motion, parameters of the catamaran structure are described as demi-hull separation (S), breadth of demi-hull (B), height of catamaran (H), length overall (L), and draft (T). In addition, the catamaran supports a turbine that has a diameter (D) and a span length (Ls). The demi-hull separation (S) is measured between the inner sides of the demi-hull. The data of each of these parameters is shown in Table 1 and depicted at Figs. 1 and 2.

The base structure has three configurations. First, the catamaran structure is without a turbine load (Fig. 1(a)). Second, the catamaran structure supports a single turbine load (Fig. 1(b)). Third, the catamaran supports twin turbines load (Fig. 1(c)). In the third condition, twin turbines are arranged in canard position (Li 2014). Antheaume *et al.* (2008) report that the closer the turbine distance is, the higher turbine power efficiency will be. The distance between the turbines in the third condition is 1.5D (Antheaume *et al.* 2008) and illustrated in Fig. 1(c). This distance is measured from the rotor shaft axis of first turbine to the rotor shaft axis of second turbine (Antheaume *et al.* 2008). The turbines have co-rotating configuration designed to generate total turbine power of 50 kW with a rated current speed of 1.3 m/s.

Table 1 Parameters of catamaran as power station

Parameter	Symbol	Value	Unit
Demi-hull separation	S	9.9	m
Breadth of demi-hull	B	2	m
Height of catamaran	H	3	m
Catamaran length	L	24	m
Draft	T	1.2	m
Diameter of turbine	D	4	m
Length of span	Ls	5.5	m

Table 2 Performance parameters

Parameters	Catamaran Without Turbine	Single Turbine-loaded Catamaran	Twin Turbines- loaded Catamaran
Total Weight (kg)	90,660	104,360	118,060
$K_{xx}$ (m)	1.14	1.17	1.19
$K_{yy}$ (m)	1.14	1.17	1.19
$K_{zz}$ (m)	0.01	0.01	0.02

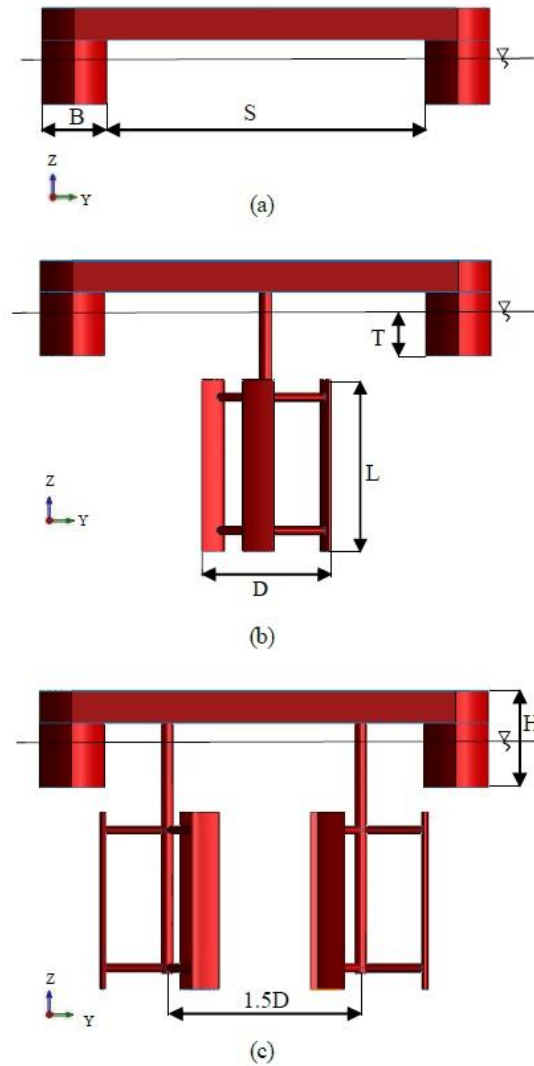


Fig. 1 Catamaran configuration without turbine (a), with single turbine (b), and with twin turbines (c)

The turbines are conditioned as dead weight which these do not rotate. The performance parameters for each condition are described on total weight and radius of gyration for rolling ( $K_{xx}$ ), pitching ( $K_{yy}$ ) and yawing ( $K_{zz}$ ) shown in Table 2.

To solve the problem, twin turbines-loaded catamaran was simulated by the ratios of the demi-hull separation ( $S$ ) to the breadth of demi-hull ( $B$ ),  $S/B$ , where the breadth of demi-hull was constant. The variations of ratio,  $S/B$ , are 3.45, 4.95, 6.45, 7.2 and 7.95 where  $S/B$  of 4.95 is the base structure. Moreover, the value of the draft ( $T$ ), height of the catamaran ( $H$ ), length overall ( $L$ ), and the size of the turbine are assumed to be constant. In order to have cases comparable to those of previous works in the literature, e.g., Jones (1972), this study considers regular waves with the height

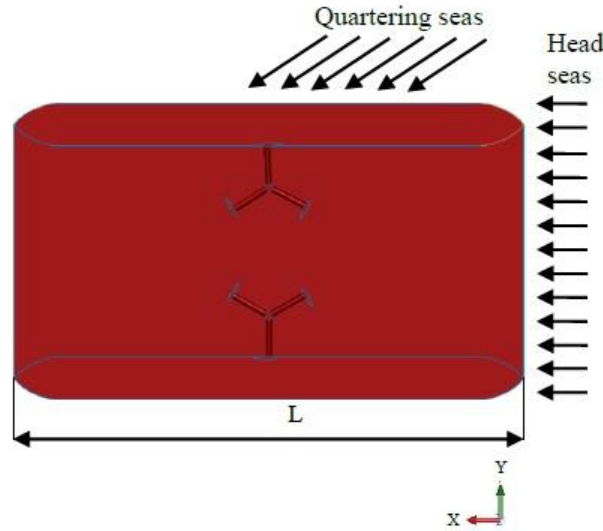


Fig. 2 Catamaran with incident wave direction on the bottom view

of 0.8 m. The incident waves are from the head seas (0 rad) and quartering seas (0.79 rad) (Fig. 2). The motion response analysis is continued with irregular wave approaching the real sea conditions which has a potential tidal current energy. The environmental conditions are with significant wave height of about 0.09 to 1.5 m and the wave period,  $T$ , of about 1.5 to 6 s or corresponding to the wave frequency,  $\omega$ , of about 1.1 to 4.2 rad/s.

### 3. Numerical simulation of motion

CFD calculates the motion response using the equation which is explained in this section. These calculations analyze hydrodynamics and wave impact using potential flow solver. The basic equation (Eq. (1)) is correlated with six-degrees-of-freedom (6-DOF) of RAO (Kim *et al.* 2015, Junianto *et al.* 2018a). The subscription  $i$  in this equation shows every modes of motion such as surge, sway, heave, roll, pitch and yaw. The 6-DOF of motion may be more accurate in numerical simulations in which the equation of motion and diffraction force equation are used (Kim *et al.* 2015).

$$(M_s + M_a)\ddot{x}_i + C\dot{x}_i + K(t) = F_i \quad (1)$$

Structural mass ( $M_s$ ), added mass ( $M_a$ ), damping coefficient ( $C$ ), stability coefficient ( $K$ ) are the parameters of radiation force and external force ( $F_i$ ) is the parameter of diffraction force to calculate in motion responses. Phase angle parameters of 6-DOF or wave exciting force are defined with the differences from the time when the wave peak is at the center of gravity of the catamaran structure to reach its peak value. In other words, the incident waves elevation ( $\zeta_0$ ) and response parameters of 6-DOF ( $\zeta_{k0}$ ) are defined according to Eqs. (2) and (3).

$$\zeta_0 = a_w \cos(-\omega t + \alpha) \quad (2)$$

$$\zeta_{k0} = a_p \cos(-\omega t + \alpha + \vartheta) \quad (3)$$

Where  $a_w$  is the regular waves amplitude,  $\omega$  is the wave frequency (in rad/s),  $\alpha$  is the wave phase angle (in radians) relative to the origin of the fixed reference axes,  $a_p$  is the amplitude of the parameters of 6-DOF, and  $\vartheta$  is the phase angle of the parameters of 6-DOF (in rad/s). The phase angle in degrees is given by Eq. (4).

$$\vartheta = \frac{360}{2\pi} \omega dt \quad (4)$$

The 6-DOF of motion in RAO information is presented in the form of non-dimensional curves. The abscissa axis is the ratio of the wavelength ( $\lambda$ ) to the catamaran length of the catamaran ( $L$ ),  $\lambda/L$ . To show the result, the ordinate axis is RAO (Eq. (5)) in non-dimensional form.

$$RAO = \frac{\zeta_{k0}}{\zeta_0} \quad (5)$$

RAO for translation motion in the form of surge, sway and heave are the direct ratio between the amplitude of the motion,  $\zeta_{k0}$  (in units of length), and the incident wave amplitude,  $\zeta_0$  (in units of length), displayed by Eq. (5). The non-dimensional response or RAO for rotational motion (Eq. (6)) such as roll, pitch and yaw are the comparison between the amplitude of the motion (in radian) and the slope of the wave which is the multiplication of the amplitude of the incident waves with the wave number,  $k_w$ , (Eq. (7)), where  $d$  is water depth.

$$RAO = \frac{\zeta_{k0}}{\zeta_0 k_w} \quad (6)$$

$$k_w = \left( \frac{\omega}{\sqrt{gd}} \right) \quad (7)$$

The equation is operated numerically with CFD potential flow analysis. The governing Eq. (1) to Eq. (9) are solved by a two-step hydrodynamic method. In the first step, the structures are computed by explicit computing the RAOs and pressure variations in hydrodynamic diffraction. In the second step, the setup of the first step is continued by explicit computing the wave spectra and significant amplitude responses in hydrodynamic response. The engineering tool which is used as numerical solver analyzing an integrated hydrodynamics based on 3D diffraction steps.

The geometry and physical bounds of the cases are defined as surface body. The environmental loads are regular wave, irregular wave and the uniform flow tidal currents. Other assumptions of environmental load are explained in Section 2. Typically, this analysis looks at the regulation contained in the API RP 2FPS about floating systems. The catamaran structure in numerical simulation is meshed with the boundary element method.

Mesh as a boundary becomes a small part or became elements (Junianto *et al.* 2018b). The meshing process was automatically generated in potential flow solver by inputting the defeating tolerance and maximum element size. The mesh is defined with uniform, unstructured consisting of a combination of hexahedral. Once it was generated, the results showed the number of nodes and elements meshing results. These explain a water-immersed catamaran. The number of elements which are created in this simulation cannot exceed 40,000 elements because of the solver spesification. The growth rate type is exponential set in 1.2. The meshing result is depicted at Fig. 3 and the element inputs are shown in Table 3. To get the solution, the simulation has been set in time response analysis with time step of 0.5 s for 13,500 s.

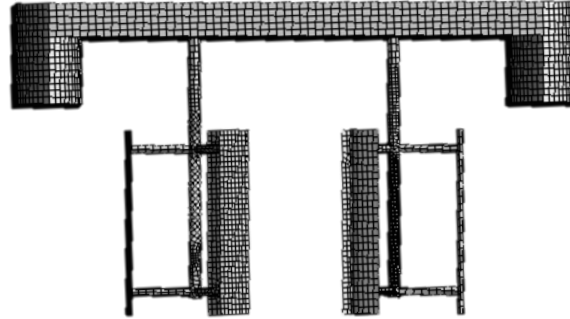


Fig. 3 Meshing of the structure

Table 3 Detail of mesh

$S/B$	Defeaturing Tolerance	Maximum Element Size	Number of Nodes	Number of Elements
4.95	0.1 m	0.4 m	24,873	24,943
3.45	0.1 m	0.4 m	21,146	21,209
6.45	0.1 m	0.4 m	23,122	23,192
7.2	0.1 m	0.4 m	26,396	26,457
7.95	0.1 m	0.4 m	28,082	28,144

The motion response in regular wave is shown as an RAO. The peak of RAO indicates the resonance which is the similar value between natural frequency of the structure and frequency of the ocean waves (Mukhtasor *et al.* 2016). The catamaran is further calculated in irregular wave conditions. The wave spectrum ( $S_j(\omega)$ ) is calculated by ITTC equation (Eq. (8)). To get response spectrum, RAO is squared and multiplied by ITTC wave spectrum. These parameters are calculated further to obtain a significant motion amplitude value from the catamaran (Eq. (9)).

$$S_j(\omega) = \frac{0.0081 \times g^2}{\omega^5} \cdot \exp\left(\frac{-3.11}{H_s^2 \times \omega^4}\right) \quad (8)$$

$$m_n = \int_0^\infty \omega^n S_j(\omega) d\omega \quad (9)$$

where moment spectra,  $m_n$ , denotes varian  $n^{\text{th}}$  and  $S_j(\omega)$  is the wave spectrum.

## 4. Performance analysis

### 4.1 Numerical verification

Numerical modeling is subject to various sources of uncertainty. A verification may be

undertaken by the considerations on variety of settings of the input parameters (Law and Kelton 1991, Sargent 2011). Before calculating the motion response and force per area for each variation of the case, the first stage is a verification of the numerical program.

This verification process was carried out by using a case in the experiment of a single-turbine-loaded catamaran as per Ma *et al.* (2016). The catamaran is scaled in a ratio of 3:40 as the basis of the floating structure. The experiment was carried out by time domain which the data has been shown in maximum value per time response. The data on the maximum pitch RAO while the turbine does not rotate (Fig. 4) is used to in this verification.

At the ratio of wavelength to catamaran length of 1.8 (Fig. 4), the maximum pitch RAO of the experiment is 1.38 deg/cm. While the numerical results show that the maximum pitch RAO is 1.44 deg/cm (or, the difference is 4.54%). Then, the lowest difference of 2.98% occurs at the ratio of wavelength to catamaran length of 1.2. The overall results of this comparison have the difference ranging from 2.98% - 7.17% and this shows a good agreement between the numerical and the experiment.

#### 4.2 Effects of the presence of the turbines

Floating structures will have different behaviors when they have different loading, even though the structure type is the same, including a catamaran. Adding turbine loads will change the catamaran behavior. In studying RAO characteristics of turbine-loaded catamaran, three configurations were considered, i.e., catamaran without turbine, single turbine-loaded catamaran and twin turbines-loaded catamaran. For cases with environmental loads described in the previous section, numerical modeling has been conducted in regular wave and shown in Figs. 5 and 6.

The surge RAO characteristics in head seas can be seen in Fig. 5a. The surge RAO increases following the wavelength increment after  $\lambda/L$  of 0.44. Then, the surge RAO of catamaran has reduction following the number of turbines. For example, at the  $\lambda/L$  of 3.35, surge RAO has value of 3.29 m/m for the catamaran without turbine, 2.91 m/m for the single turbine-loaded catamaran and 2.67 m/m for the twin turbines-loaded catamaran.

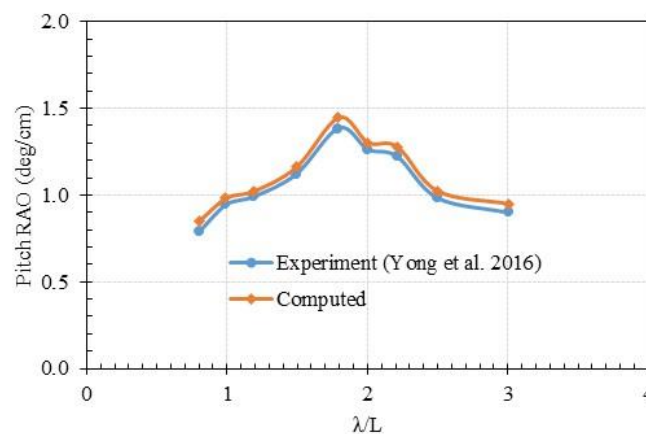


Fig. 4 Comparison maximum pitch angle curve (catamaran single turbine)

The addition of turbine mass changes the total weight of the structure and the wave excitation force decreases. The characteristic of the surge RAO curve is a motion response without stiffness. Thence, in this mode of motion response, it does not have a peak of resonance. A peak at the  $\lambda/L$  of 0.23 is due to the coupling effect with pitch motion.

Horizontal-translation motion on the imaginary axis Y (Fig. 5(b)), Sway, has the similar curves with surge motion. The sway RAO rises when the ocean waves come from the direction of the beam seas. Because the potential location is on the strait, the incoming waves from side of catamaran are rarely. In the head seas, it does not give a significant effect to the catamaran, because almost all  $\lambda/L$  have no RAO and the peaks are very small and can be ignored. In the quartering seas (Fig. 5(b)), sway RAO has value of 2.07 m/m for the catamaran without turbine, 1.99 m/m for the single turbine-loaded catamaran, and 1.89 m/m for the twin turbines-loaded catamaran.

Heave RAO in Fig. 5(c) shows the value of 1 m/m for all types of configuration after  $\lambda/L$  of 1.32 for all directions of incoming waves. This is in accordance with the contouring conditions which the motion of catamaran follows the elevation of the wave because of the long wavelength. Then, heave RAO gradually decreases at the  $\lambda/L$  of 1.1. The small peak at the low  $\lambda/L$  is caused by the resonant frequency of pitch motion (Fig. 6b) while there is an effect of pitch coupling motion on heave.

The big effect of pitch on heave RAO is in head seas (Fig. 5(c)). At  $\lambda/L$  of 0.35, the catamaran without turbine has heave RAO of 0.29 m/m, the single turbine-loaded catamaran has heave RAO of 0.42 m/m and the twin turbines-loaded catamaran has heave RAO of 0.51 m/m. The twin turbines-loaded catamaran has the highest heave RAO at  $\lambda/L$  of 0.35 because the total weight of the structure is the biggest. Hence, twin turbines-loaded catamaran is drowned deeper.

Roll RAO has a high value when the waves are in the quartering seas condition. However, when the incoming waves are from head seas, the roll RAO is relatively closed to 0 rad/rad. In Fig. 6(a), roll RAO has relatively constant after  $\lambda/L$  of 1.32. There is no significant difference between the roll RAO of three configurations on quartering seas after  $\lambda/L$  of 0.5.

The pitch RAO curve in Fig. 6(b) increases significantly after  $\lambda/L$  of 0.36 and the peak is at  $\lambda/L$  of 0.65. Then, pitch RAO moves downward from  $\lambda/L$  of 0.44. At  $\lambda/L$  of 0.31, the catamaran without turbine has value of 0.14 rad/rad, the single turbine-loaded catamaran value of 0.15 rad/rad, and the twin turbines-loaded catamaran has value of 0.18 rad/rad. In the head seas condition, the lowest RAO pitch at  $\lambda/L$  of 0.36 is catamaran without turbine.

The yaw RAO in Fig. 6(c) has different results than yaw in general. At the high  $\lambda/L$  ratio, The turbine-loaded catamaran has rising yaw RAOs in head seas. However, catamaran without turbine follows the principle of yaw motion in theory which has a high value when quartering seas. In the rotational motion, catamaran without turbine has the lowest RAO because it has a symmetric configuration and low damping moment. Because of the turbine, catamaran changes the displacement value and increases the RAOs.

The RAOs (Figs. 5 and 6) show that the turbine-loaded catamaran gives different behavior of motion response compared to catamaran without turbine. The twin turbines-loaded catamaran which increases power turbine capacity in single of platform has relative high rotational RAO. The efforts to vary the demi-hull distance are to decrease the RAO.

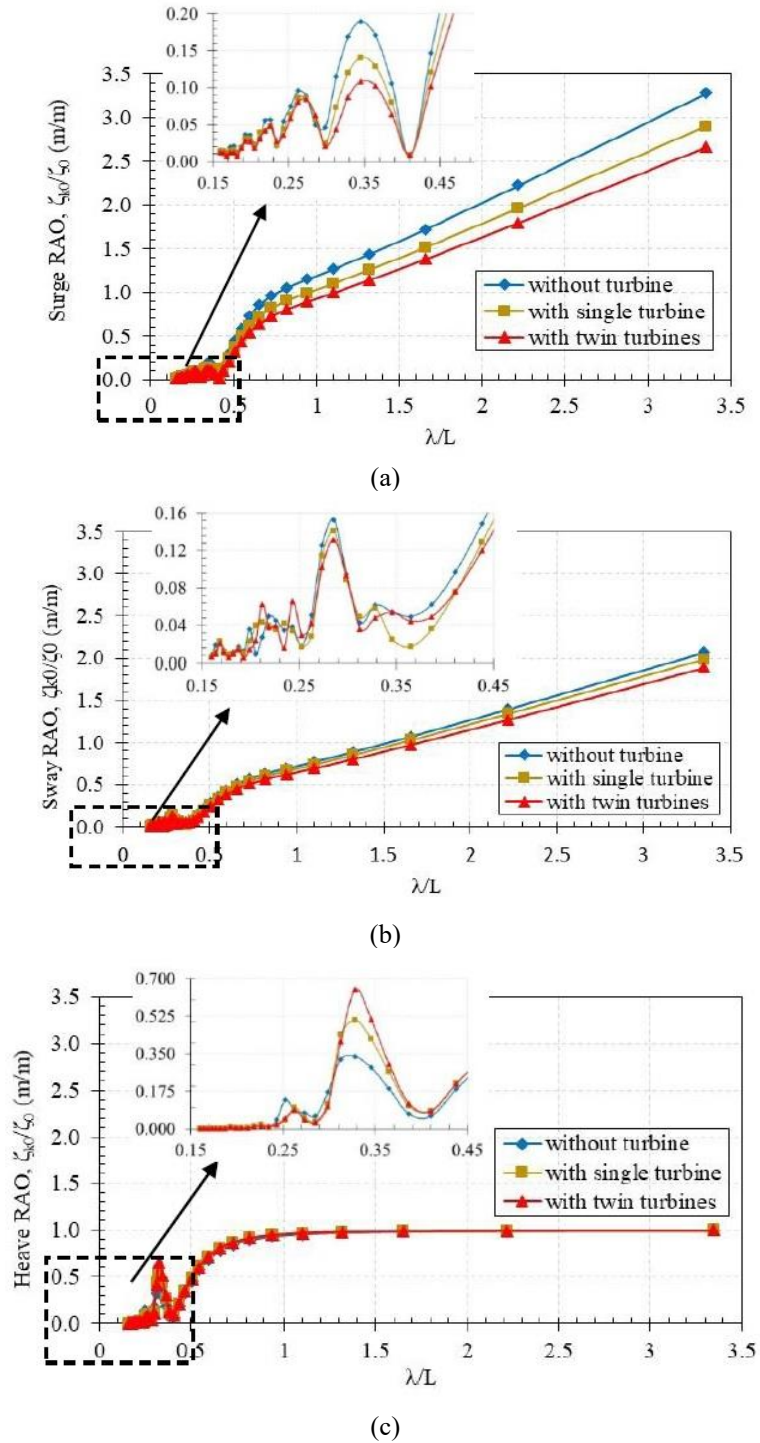
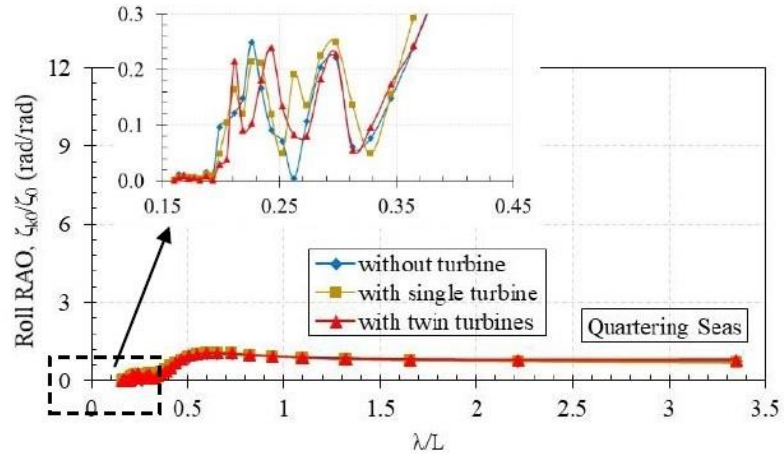
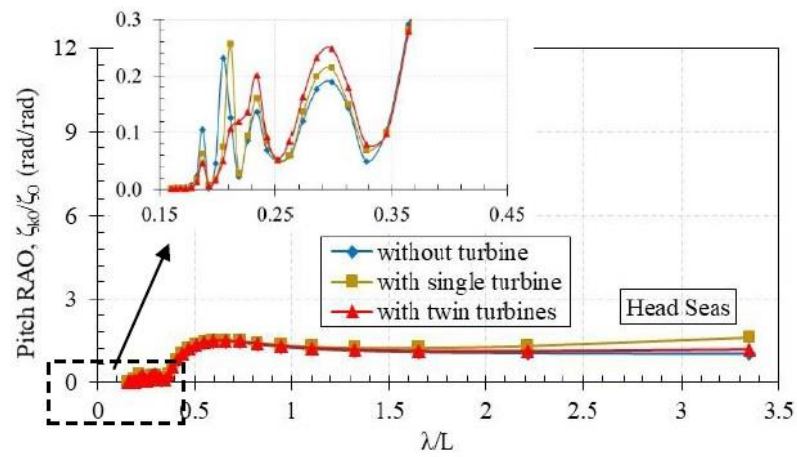


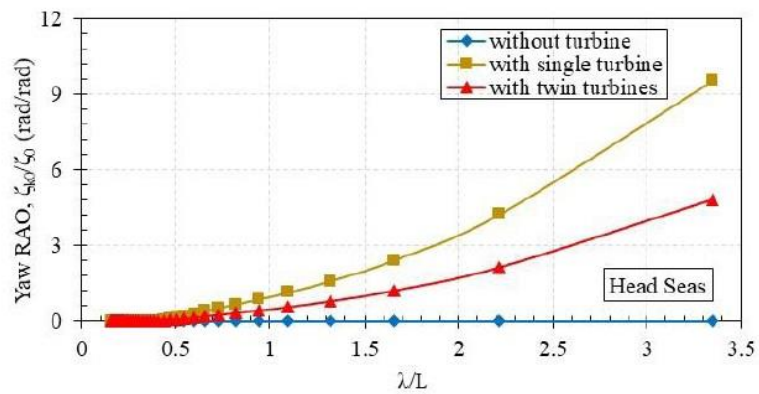
Fig. 5 Non-dimensional RAO surge in head seas (a), sway in quartering seas (b) and heave in head seas (c)



(a)



(b)



(c)

Fig. 6 Non-dimensional RAO of roll (a), pitch (b) and yaw (c)

### 4.3 Effects of parametric variations in regular wave

The twin turbines-loaded catamaran has relative high RAO. The RAO is reduced by giving variation of separation of demi-hull. The base case is the ratio of the demi-hull separation to the breadth of demi-hull ( $S/B$ ) of 4.95. Then the cases are 3.45, 6.45, 7.2 and 7.95 which is showed. The  $S/B$  ratio after 7.95 has been checked and has identical results with the ratio, for that reason the results are not considered in this analysis.

The effect of change the separation of demi-hull are shown in Figs. 7 and 8. The graphs are presented in non-dimensional form consisting of head seas and quartering seas conditions. In the RAO calculation, the wave load is regular waves. The results show the resonance between the supporting structure and the ocean waves.

The variations of the demi-hull separation have effect on the translational motion (Fig. 7) which are surge, sway and heave motion. In head seas, the ratio variations of  $S/B$  have the significant effect of surge in the smallest and the largest ratio. At the quartering seas, the parametric variations of  $S/B$  changes the natural frequency of the catamaran, especially sway motion. Then, heave RAO is associated by the rotational-vertical motion, pitch RAO.

Moreover, the results of changes in the parametric ratio also have the effect on the rotational motion of the catamaran (Fig. 8) which are roll, pitch and yaw. The high RAOs are roll RAO in quartering seas, pitch RAO in head seas and yaw RAO in quartering seas. According to Ma *et al.* (2018), rotational RAO is an important parameter in maintaining turbine efficiency. Therefore these parameters are further analyzed. Low RAOs are on  $S/B$  of 3.45, 7.2, 7.95. However the RAO of  $S/B$  of 3.45 ratio is ignored because it is not consistent in producing low RAO. In addition, the RAO of  $S/B$  of 7.95 has identical results with the  $S/B$  of 7.2. Therefore, the ratio of  $S/B$  of 4.95 and 7.2 is analyzed in irregular wave.

Furthermore, the incoming waves which affect the performance of the twin turbines-loaded catamaran generate pressure on the structure. In this case study, the variations on the separation of demi-hull have the various results in pressure. Thus, the distribution of pressure values that occur on the surface of the catamaran with  $S/B$  of 7.2 can be seen in Fig. 9 to Fig. 10. And, for other conditions of catamaran variations, it has the similar pattern on pressure distribution however the amount of pressure is different. The catamaran with  $S/B$  of 7.2 is the structure starting the low RAO.

### 4.4 Effects of significant wave on significant amplitude

The  $S/B$  variations of the twin turbines-loaded catamaran generally have two RAO patterns. These patterns are represented by  $S/B$  of 4.95 as the base case and  $S/B$  of 7.2 as the new parameter ratio. The  $S/B$  of 7.2 is the ratio which starts the decrease of the RAO at each ratio of  $\lambda/L$ . The both of  $S/B$  ratios produce different response spectra for pitch, roll and yaw motions. The difference is due to dissimilarities in natural frequencies between twin turbines-loaded catamaran with  $S/B$  of 4.95 and  $S/B$  of 7.2.

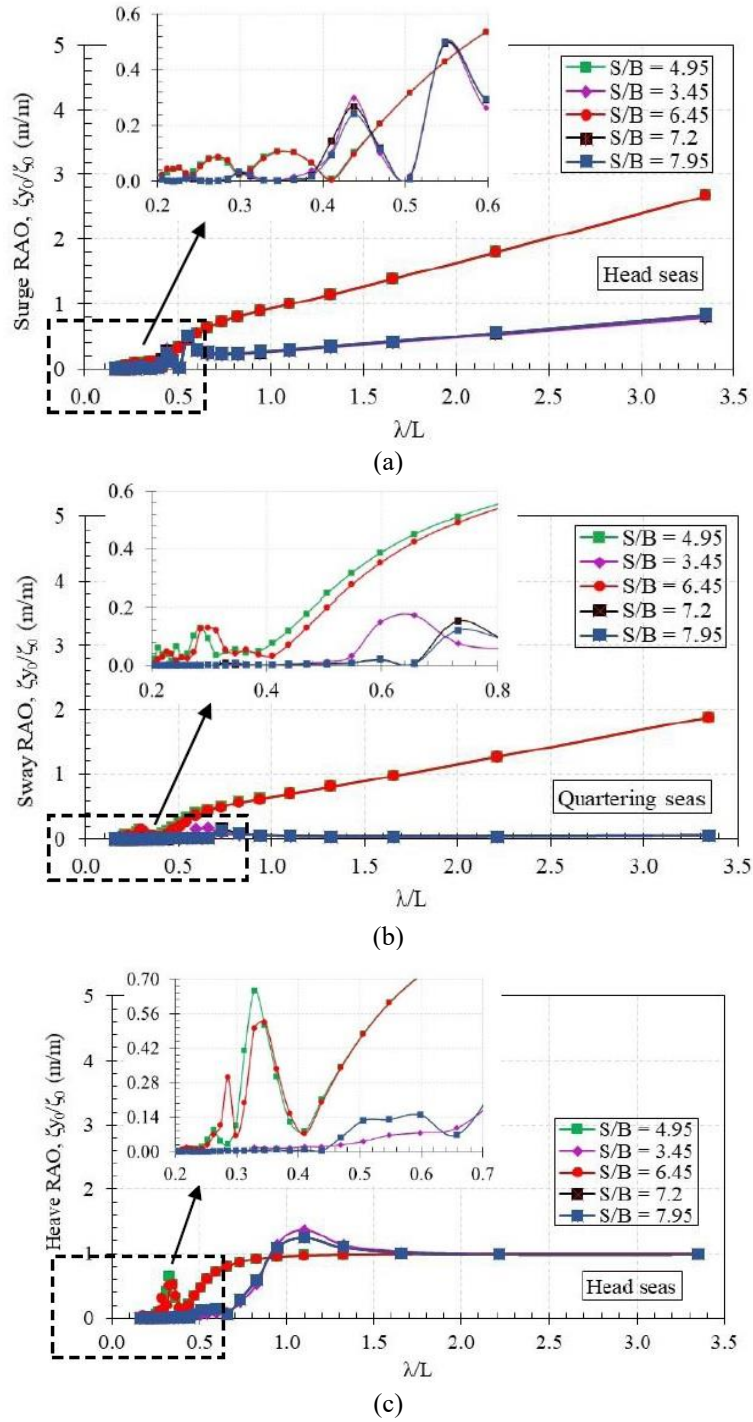
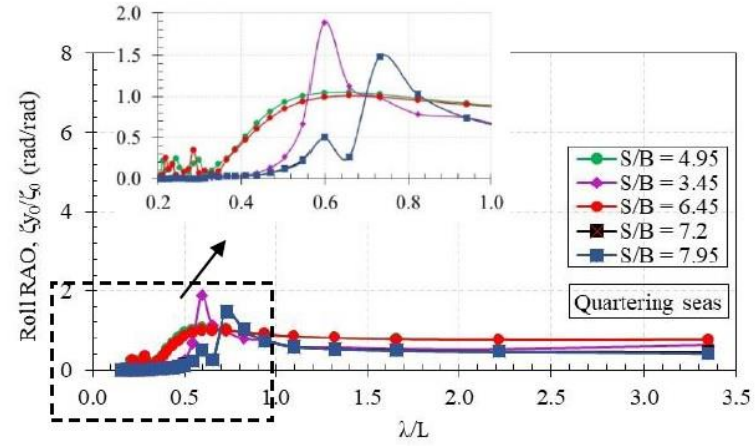
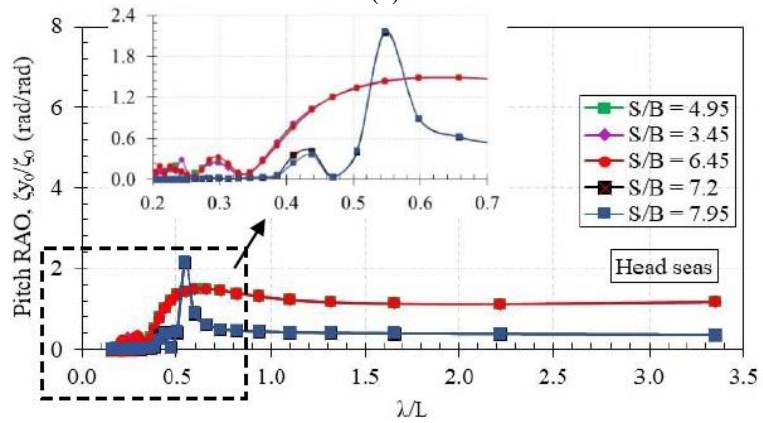


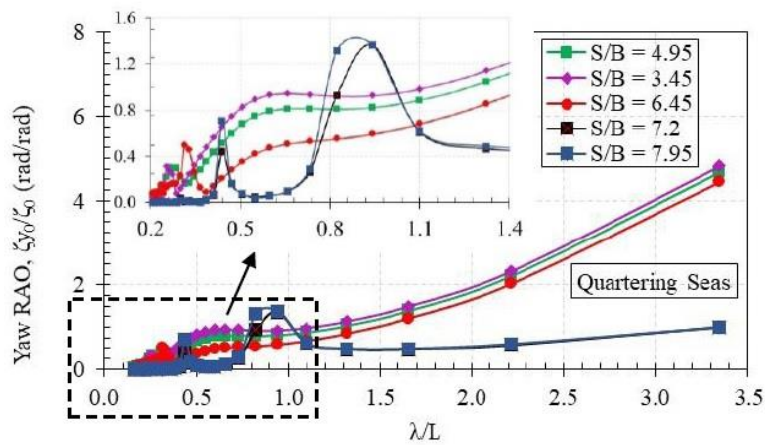
Fig. 7 Non-dimensional translational RAO characteristics on surge (a), sway (b) and heave (c)



(a)



(b)



(c)

Fig. 8 Non-dimensional rotational RAO characteristics on roll (a), pitch (b) and yaw (c)

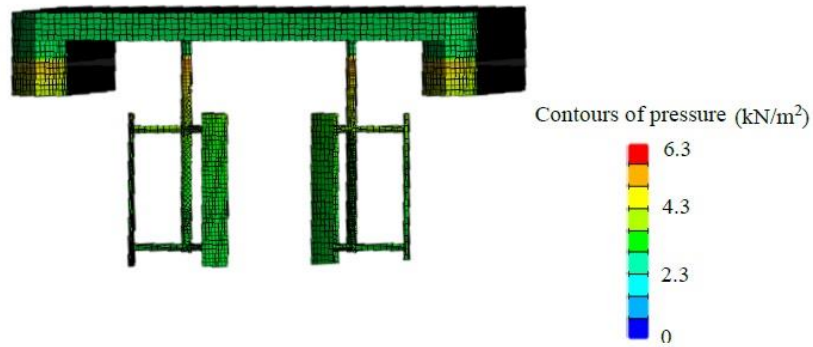


Fig. 9 Pressure distribution on turbines-loaded catamaran at head seas

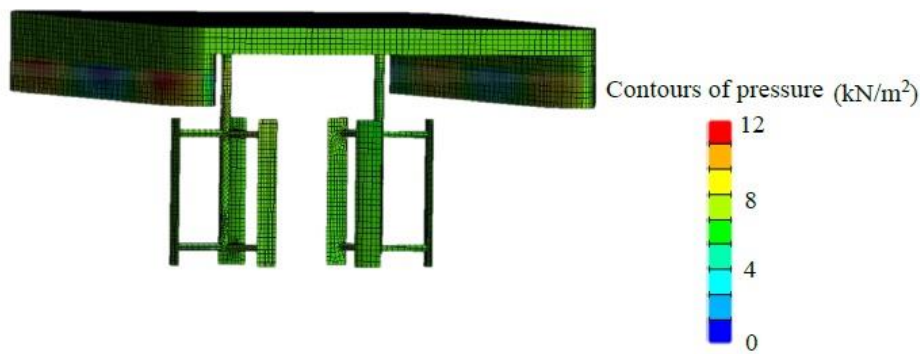


Fig. 10 Pressure distribution on turbines-loaded catamaran at quartering seas

In the previous section, RAOs of  $S/B$  of 7.2 have the new natural frequency. This case has lower RAO than base case ( $S/B$  of 4.95) at the range after the resonance condition. The RAO value is not enough to decide that  $S/B$  of 7.2 is better than  $S/B$  of 4.95. Therefore, it is necessary to analyze the motion response on an irregular wave where the  $S/B$  parameters are compared by significant wave height ( $H_s$ ) variations.

Irregular wave has a spectral density which is influenced by significant wave height. The spectra are calculated using the ITTC method. In this case, the resulting wave spectrum is affected by significant wave height from 0.09 to 1.5 m (Fig. 11). The variation of the significant waves is a sample that might occur in the strait waters.

Fig. 11 shows that there is a wave spectrum peak change over from the small ratio of  $\lambda/L$  to the large ratio of  $\lambda/L$ . In the graph, the peak of the wave spectrum is greater along with the increase in  $H_s$ . The peak increases gradually in the range of  $1.7 \times 10^{-4}$  to  $0.2 \text{ m}^2/(\text{rad/s})$ . The graph also explains that the wave spectrum curve has a wide shape on the variations of  $H_s$ . In other words, the wave energy is generated by the wide range of  $\lambda/L$  ratios.

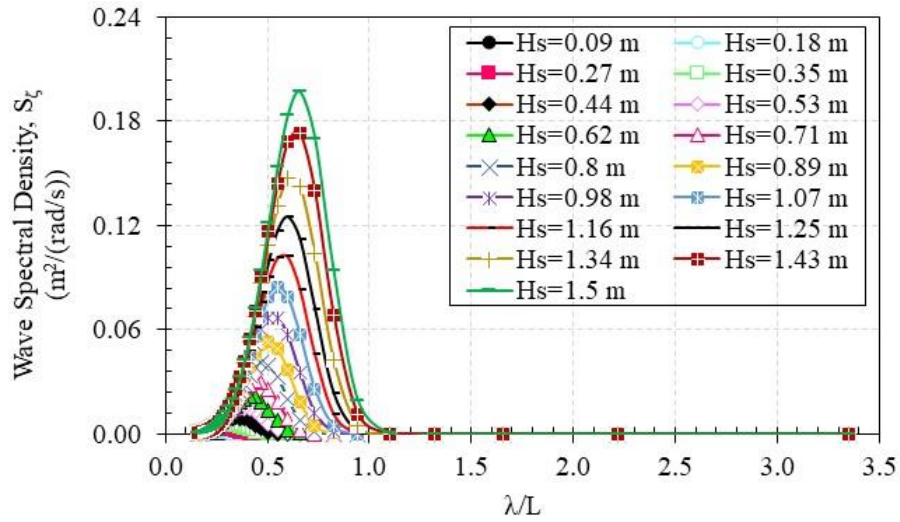
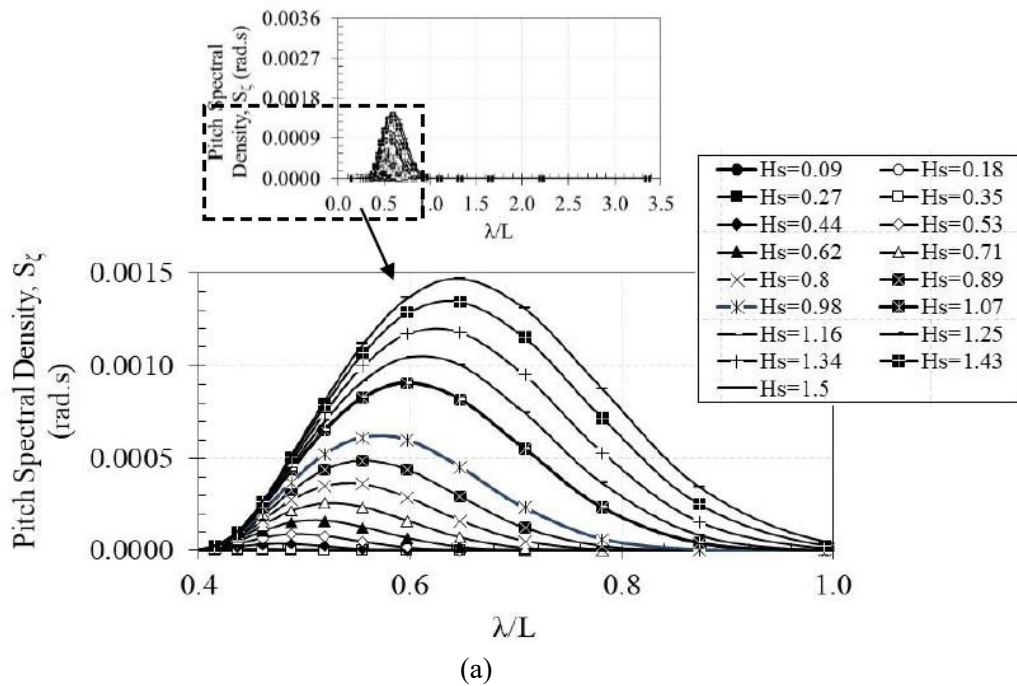


Fig. 11 The effect of significant wave height changes on ITTC wave spectral density



(a)  
Continued-

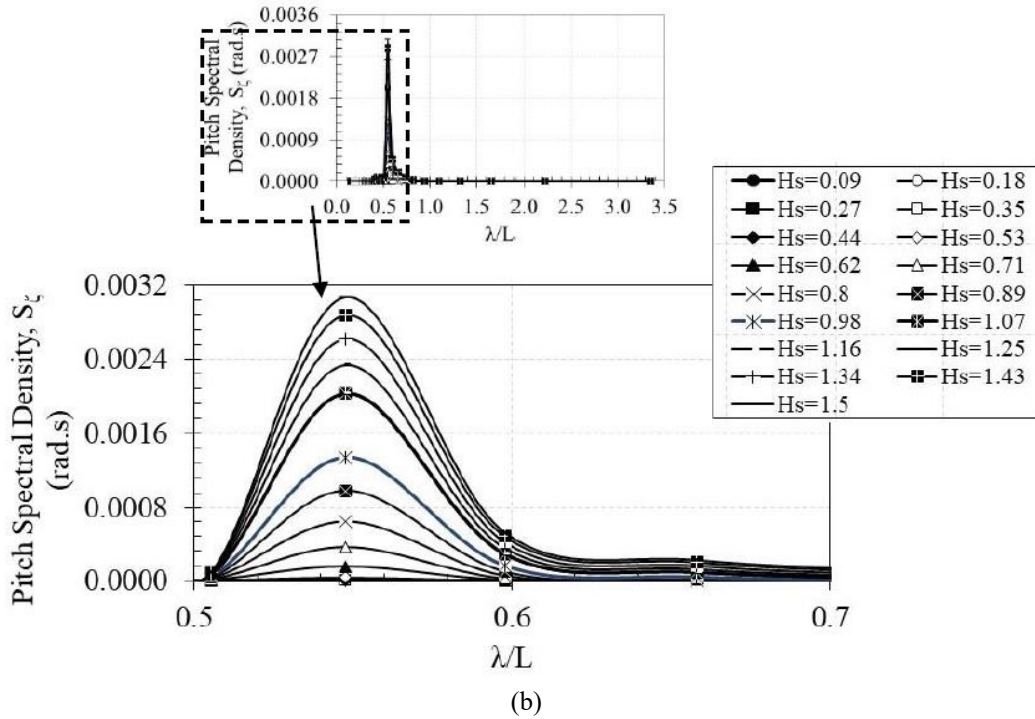


Fig. 12 Pitch response spectrum of twin turbines-loaded catamaran with  $S/B$  of 4.95 (a) and 7.2 (b) in head seas

The rotational motion of the twin turbines-loaded catamaran is a major concern in this paper. The motion is a significant parameter which causes turbine efficiency decrease (Wang *et al.* 2016, Ma *et al.* 2018). The rotational response spectrum is influenced by wave spectrum and RAO. Therefore, pitch, roll and yaw motion is a comparative parameter between catamaran with  $S/B$  of 4.95 and  $S/B$  of 7.2. Response spectrum graphs of rotational motion are shown in Figs. 12 to 14. The graphs show the linearity between the increase in  $H_s$  and the increase in response spectrum of rotational motion.

The twin turbines-loaded catamaran with  $S/B$  of 4.95 has the response spectrum of the rotational motion which is similar to the wave spectrum. The pitch response spectrum (Fig. 12(a)) has higher peak value than the roll response spectrum (Fig. 13(a)) at the same significant wave height, *e.g.*,  $H_s$  of 1.16 m. The peak of the pitch response spectrum is 0.0009 rad.s while the of the roll response spectrum is 0.0004 rad.s. In this  $H_s$ , the yaw response spectrum has peak response of 0.0002 (Fig. 14(a)). The response spectra explain that the catamaran does not face an acute resonance because these are smaller than wave spectra.

The response spectra of the rotational motion catamaran with  $S/B$  of 7.2 are shown in Figs. 12(b), 13(b) and 14(b). The graphs of the response spectrum of the motions have a leaner shape compared to the graph of the wave spectrum (Fig. 11).

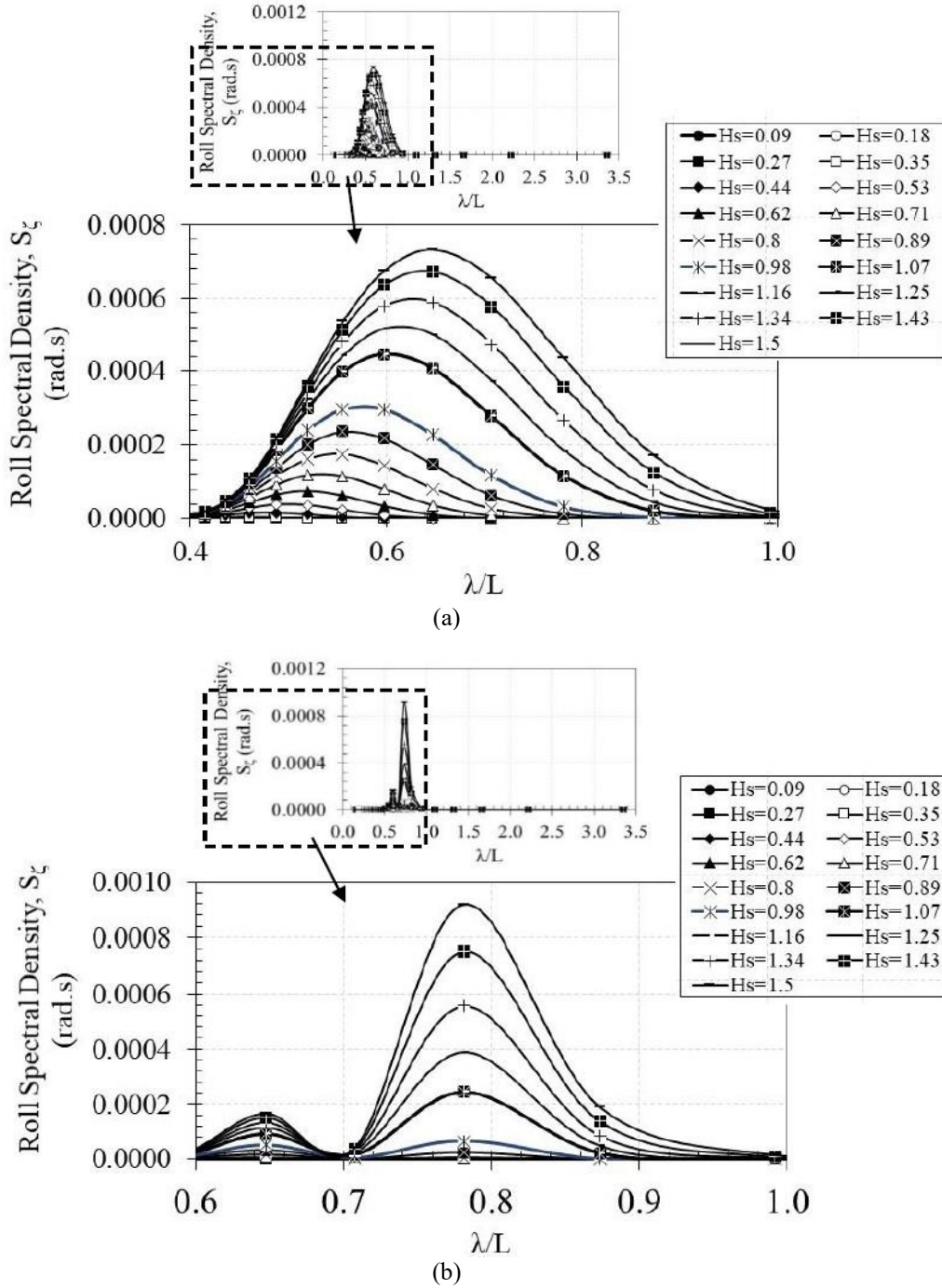


Fig. 13 Roll response spectrum of twin turbines-loaded catamaran with  $S/B$  of 4.95 (a) and 7.2 (b) in quartering seas

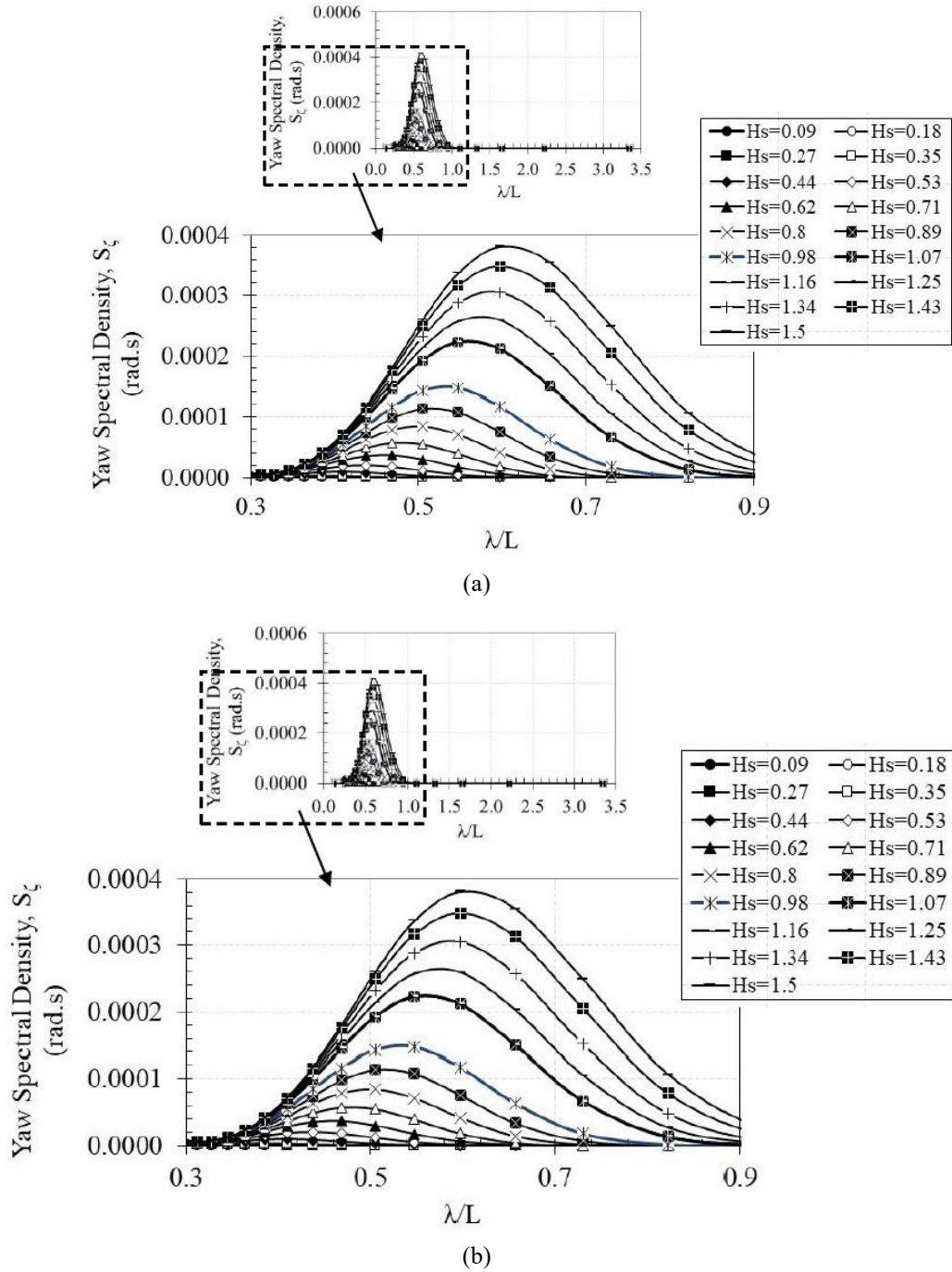
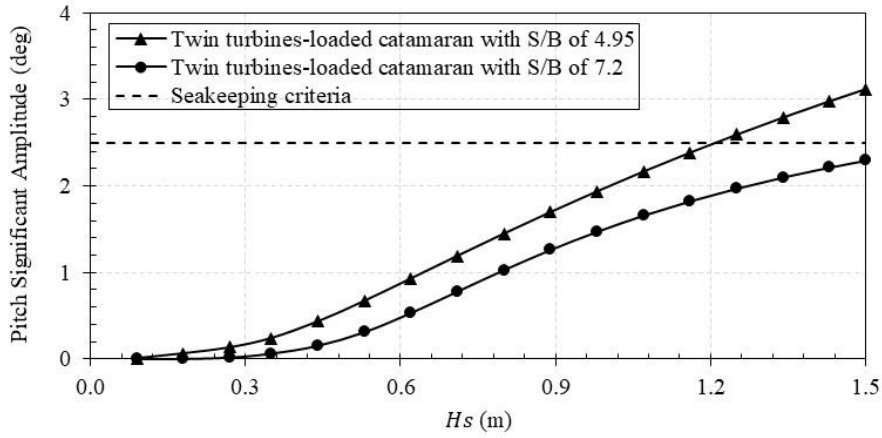
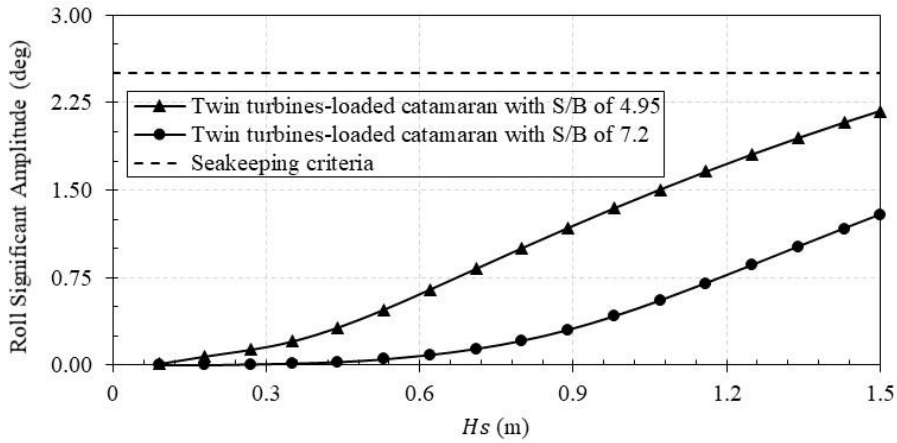


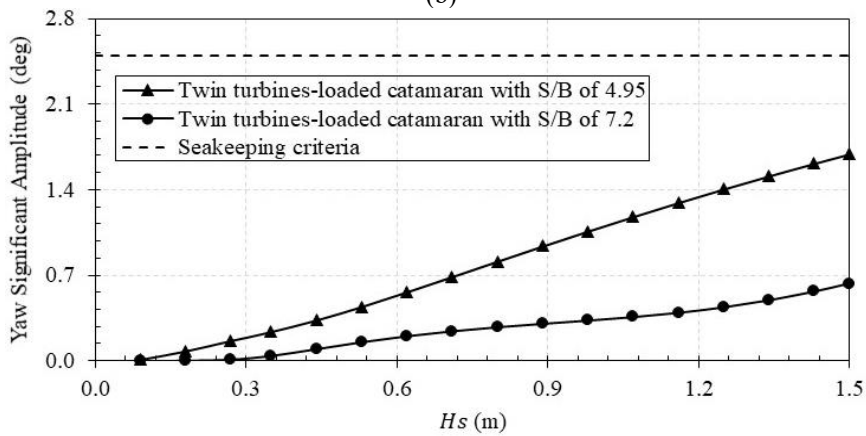
Fig. 14 Yaw response spectrum of twin turbines-loaded Catamaran with  $S/B$  of 4.95 (a) and 7.2 (b) in quartering seas



(a)



(b)



(c)

Fig. 15 Significant amplitude of rotational motion on Pitch (a) in head seas, Roll (b) and Yaw (c) in quartering seas

Table 4 Performance comparison

Parameters	Maximum Righting Arm (m)	Maximum Righting Moment (kN.m)
$S/B$ of 4.95	2.5 (Jing <i>et al.</i> 2013, Qasim <i>et al.</i> 2018)	295.15 (Jing <i>et al.</i> 2013, Qasim <i>et al.</i> 2018)
$S/B$ of 7.2	1.5	177.09

The slender curve is due to the contribution of the peak of RAO and the natural frequency of the catamaran with  $S/B$  of 7.2. The ratio has more damping force so that the spectrum produces small area under the curve. The peak values of pitch (Fig. 12(b)), roll (Fig. 13(b)) and yaw (Fig. 14(b)) response spectra at  $H_s$  of 1.16 m respectively are 0.002 rad.s, 0.0002 rad.s and 0.0001 rad.s. The pitch and roll response spectra of  $S/B$  of 7.2 are the greatest. However, the yaw response spectrum of  $S/B$  of 7.2 is the smallest.

After analyzing the response spectrum of each rotational motion, the catamarans are analyzed in the significant amplitude response. This parameter is shown in Fig. 15. In this paper, the parameter is significant amplitude which is an evaluation of dominant motions in the catamaran. The results which are influenced by significant wave height show differences between catamaran with  $S/B$  of 4.95 and 7.2.

Figs. 15(a)-15(c) show which catamaran with  $S/B$  of 7.2 has the smallest significant amplitude of pitch, roll, and yaw. The  $S/B$  ratio of 7.2 gives a decrease in pitch degree of about 26 to 98% for each significant wave height effect (Fig. 15(a)). In addition, the ratio also decreases the degree of roll motion (Fig. 15(b)) around 40 to 99%. And yaw motion (Fig. 15(c)) decreases around 62 to 98%.

The catamaran with  $S/B$  of 7.2 has the smallest degree of rotational motion. This decrease can improve the performance of twin turbines in the catamaran. In Fig. 15, there are seakeeping criteria (Molland 2008) which indicate the maximum limit in considering comfort when the catamaran operates. The motion of the catamaran with  $S/B$  of 7.2 is relatively comfortable in the range  $H_s$  of about 0.09-1.5 m.

In general, for the case catamaran at the strait, the addition of the number of turbines in twin configuration has effects. First, the turbine power capacity may increase in the single catamaran-type platform. Second, the response is lower than the single turbine-loaded catamaran. In other hand, the roll motion of the twin turbines-loaded catamaran is the highest, as the result further analysis is needed to find the lower motion with changing the distance between demi-hull. The further analysis is to compare the righting moment reported by Jing *et al.* (2013) and Qasim *et al.* (2018). Comparison of this value can be observed in Table 4. The smaller the value of the righting moment, the catamaran has relatively good stability. In other words, the catamaran with  $S/B$  of 7.2 has better stability than the the catamaran with  $S/B$  of 4.95.

## 5. Conclusions

The number of the turbines may increase the turbine efficiency in the single catamaran-typed platform. These can decrease surge and sway motion, increase heave motion, significantly increase yaw motion and slightly changes the fluctuation RAO of roll and pitch. In general, the twin turbines-loaded catamaran has lower motion than the single turbine-loaded.

Another of to find lower motion of the twin turbines-loaded catamaran is with varying the demi-hull separation ratios ( $S/B$ ). This analysis is in regular wave and gives the pattern of RAO of  $S/B$  of 4.95, 3.45, 6.45, 7.2, and 7.95. This paper shows the case of  $S/B$  of 7.2 and 7.9 being the new parameter which has lower RAO. However the  $S/B$  of 7.2 is the most acceptable because the  $S/B$  of 7.95, the widest deck, needs higher cost than  $S/B$  of 7.2.

In addition, the rotational motion responses of twin turbines-loaded with  $S/B$  of 7.2 and 4.95 are compared in irregular wave. The rotational motion amplitude increment follows the  $H_s$  increment. The  $S/B$  of 7.2 has roll motion about of 25.6% of the  $S/B$  of 4.95. In pitch degree, the  $S/B$  of 7.2 has motion response about of 54.4% of the  $S/B$  of 4.95. And, the  $S/B$  of 7.2 has yaw motion about of 27.3% of the  $S/B$  of 4.95.

In the conclusion, the catamaran motion response with the twin turbines load becomes lower in which the demi-hull distance is 7.2 times its breadth. The results might be applicable on the tidal current energy potential site. In the future, the mooring configuration may be included in another study that may be expected to give more damping effect.

## Acknowledgements

The authors would like to convey a great appreciation to the Directorate General of Resources for Science, Technology and Higher Education; Ministry of Research, Technology and Higher Education of the Republic of Indonesia for granting the scholarship and the project under schemes called The Education of Master Degree Leading to Doctoral Program for Excellent Bachelor (PMDSU) and Competency Funding Scheme (Hikom).

## References

- Antheaume, S., Maitre, T. and Achard, J.L. (2008), "Hydraulic darrieus efficiency for free flow fluid condition versus power farms conditions", *Renew. Energ.*, **33**, 2186-2198. <https://doi.org/10.1016/j.renene.2007.12.022>.
- Bachant, P. and Wosnik, M. (2015), "Performance measurements of cylindrical- and spherical- helical cross-flow marine hydrokinetic turbines, with estimates of energy efficiency", *Renew. Energ.*, **74**, 318-325. <https://doi.org/10.1016/j.renene.2014.07.049>.
- Centeno, R., Varyani, K.S., Soares, C.G. (2001), "Experimental study on the influence of hull spacing on hard-chine catamaran motions", *J. Ship Res.*, **45**(3), 216-227.
- Danisman, D.B. (2014), "Reduction of demi-hull wave interference resistance in fast displacement catamarans utilizing an optimized centerbulb concept", *Ocean Eng.*, **91**, 227-234. <https://doi.org/10.1016/j.oceaneng.2014.09.018>

- Duthoit, M. and Falzarano, J. (2018), "Assessment of the potential for the design of marine renewable energy systems", *Ocean Syst. Eng.*, **8**(2), 119-166. <https://doi.org/10.12989/ose.2018.8.2.119>.
- Guo, X., Yang, J., Lu, W. and Li, X. (2018), "Dynamic responses of a floating tidal turbine with 6-DOF prescribed floater motions", *Ocean Eng.*, **165**, 426-437. <https://doi.org/10.1016/j.oceaneng.2018.07.017>.
- Jahanbakhsh, E., Panahi, R. and Seif, M.S. (2009), "Catamaran motion simulation based on moving grid technique", *J. Marine Sci. Technol.*, **17**(2), 128-136.
- Jing, F., Xiao, G., Mehmood, N. and Zhang, L. (2013), "Optimal selection of floating platform for tidal current power station", *Res. J. Appl. Sci., Eng. Technol.*, **6**(6), 1116-1121. <https://doi.org/10.19026/rjaset.6.4022>.
- Jones, H.D. (1972), "Catamaran predictions in regular waves", Research and Development Center Bethesda MD Ship Performance Department.
- Junianto, S. and Mukhtasor, Prastianto, R.W. (2018a), "An analytical approach to modeling of motion-response of floating structure for ocean renewable energy conversion system", *Appl. Mech. Mater.*, **874**, 44-49. <https://doi.org/10.4028/www.scientific.net/AMM.874.44>.
- Junianto, S. and Mukhtasor, Prastianto, R.W. (2018b), "Motion response modeling of catamaran type for floating tidal current energy conversion system in beam seas condition", *Int. J. Adv. Sci., Eng. Technol.*, **6**(1), 57-61.
- Khan, M.J., Bhuyan, G., Iqbal, M.T. and dan Quaicoe, J.E. (2009), "Hydrokinetic energy conversion systems and assessment of horizontal and vertical axis turbines for river and tidal applications: A technology status review", *Appl. Energy*, **86**, 1823-1835. <https://doi.org/10.1016/j.apenergy.2009.02.017>.
- Kim, S.S., Kim S.D., Kang, D. and Lee, J. (2015), "Study on variation in ship's forward speed under regular waves depending on rudder controller", *Int. J. Naval Architect. Ocean Eng.*, **7**, 364-374. <https://doi.org/10.1515/ijnaoe-2015-0025>.
- Law, A.M. and Kelton, W.D. (1991), *Simulation Modeling and Analysis: 2nd Ed.*, McGraw-Hill Education, Singapore.
- Li, Y. (2014), "On the definition of the power coefficient of tidal current turbines and efficiency of tidal current turbine farms", *Renew. Energ.*, **68**, 868-875. <https://doi.org/10.1016/j.renene.2013.09.020>.
- Ma, Y., Hu, C., Li, Y. and Deng, R. (2018), "Research on the hydrodynamic performance of a vertical axis current turbine with forced oscillation", *Energies*, **11**, 33-49. <https://doi.org/10.3390/en1123349>.
- Ma, Y., Li, T., Sheng, Q. and Zhang, X. (2016), "Experimental study on hydrodynamic characteristics of vertical-axis floating tidal current energy power generation device", *China Ocean Eng.*, **30**(5), 749-762. <https://doi.org/10.1007/s13344-016-1001-y>.
- Molland, A.F. (2008), *The Maritime Engineering Reference Book*, Butterworth-Heinemann, Elsevier, Amsterdam, Netherlands.
- Mukhtasor Prastianto, R.W., Arief, I.S., Guntur, H.L. and Mauludiyah Setiyawan, H. (2016), "Performance modeling of a wave energy converter: pembangkit listrik tenaga gelombang laut sistem bandulan ("PLTGL-SB")", *ARPN J. Eng. Appl. Sci.*, **11**(4), 2775-2778.
- Mukhtasor, Junianto, S. and Prastianto, R.W. (2018), "On offshore engineering rules for designing floating structure of tidal current energy conversion system", *Appl. Mech. Mater.*, **874**, 71-77. <https://doi.org/10.4028/www.scientific.net/AMM.874.71>.
- Ponsoni, L., Nichols, C., Buatois, A., Kenkhuis, J., Schmidt, C., Haas, P.D., Ober, S., Smit, M. and Nauw, J.J. (2018), "Deployment of a floating tidal energy plant in the Marsdiep inlet: resource assessment, environmental characterization and power output", *J. Marine Sci. Technol.*, **24**(3), 830-845. <https://doi.org/10.1007/s00773-018-0590-y>.
- Qasim, I., Gao, L., Peng, D. and Liu, B. (2018), "Catamaran or semi-submersible for floating platform-selection of a better design", *Proceedings of the International Conference on Energy Engineering and Environmental Protection*, Sanya, China, November.
- Rho, Y.H., Jo, C.H. and Kim, D.Y. (2014), "Optimization of mooring system for multi-arrayed tidal turbines in a strong current area", *Proceedings of the ASME 2014 33rd International Conference on Ocean, Offshore and Arctic Engineering*, California, USA, June.
- Sanchez, M., Carballo, R., Ramos, V. and Iglesias, G. (2014), "Energy production from tidal currents in an estuary: A comparative study of floating and bottom-fixed turbines" *Energy*, **77**, 802-811.

- <https://doi.org/10.1016/j.energy.2014.09.053>.
- Sargent, Robert G. (2011), "Verification and validation of simulation models", *Proceedings of the 2011 Winter Simulation Conference*, Arizona, USA, December.
- Sheng, Q., Jing, F., Zhang, L., Zhou, N., Wang, S. and Zhang, Z. (2016), "Study of the hydrodynamic derivatives of vertical-axis tidal current turbines in surge motion", *Renew. Energ.*, **96**, 366-376. <https://doi.org/10.1016/j.renene.2016.04.074>.
- Uihlein, A., Magagna, D. (2016), "Wave and tidal current energy – A review of the current state of research beyond technology", *Renewable and Sustainable Energy Reviews*, **58**, 1070-1081. <https://doi.org/10.1016/j.rser.2015.12.284>.
- Wang, K., Sun, K., Sheng, Q., Zhang, L. and Wang, S. (2016a), "The effects of yawing motion with different frequencies on the hydrodynamic performance of floating vertical-axis tidal current turbines", *Appl. Ocean Res.*, **59**, 224-235. <https://doi.org/10.1016/j.apor.2016.06.007>.
- Wang, S., Sun, K., Zhang, J. and Zhang, L. (2016b), "The effects of roll motion of the floating platform on hydrodynamics performance of horizontal-axis tidal current turbine", *J. Marine Sci. Technol.*, **22**, 259- 269. <https://doi.org/10.1007/s00773-016-0408-8>.

MK